EUROPEAN CONFERENCE ON INTEGRATED OPTICS

Integrated On-chip Light Control via Out-coupling Grating Structures for Quantum Applications

(Student paper)

Anastasiia Sorokina[1,2,*], Pascal Gehrmann[1,2], Guochun Du[3], Carl-Frederik Grimpe[3], Steffen Sauer[1,2], Elena Jordan[3], Tanja Mehlstäubler[3,4,5], and Stefanie Kroker[1,2,3]

[1]Institute of Semiconductor Technology, Technische Universität Braunschweig, Hans-Sommer-Str. 66, Braunschweig, 38106, Germany
[2]Laboratory for Emerging Nanometrology, Technische Universität Braunschweig, Langer Kamp 6a/b, Braunschweig, 38106, Germany
[3]Physikalisch-Technische Bundesanstalt, Bundesallee 100, Braunschweig, 38116, Germany
[4]Institut für Quantenoptik, Leibniz Universität Hannover, Welfengarten 1, Hannover, 30167, Germany
[5]Laboratorium für Nano- und Quantenengineering, Leibniz Universität Hannover, Welfengarten 1, Hannover, 30167, Germany
[*] a.sorokina@tu-braunschweig.de

Integrated optics are a vital approach toward scalable trapped-ion quantum computers. We present numerical results for controlling linearly polarized light with various focusing features of a µm-beam via grating structures. Furthermore, we discover a multi-wavelength addressing by optimizing the design of the structure and manipulating the beam's overlap.
Keywords: *Integrated Optics, Grating Coupler, Light Polarization, Quantum Computing*

INTRODUCTION

Integrated optics for quantum experiments on chips are an essential toolbox for the miniaturization of the setup and its robustness, allowing the realization of more complex operations and simultaneously enhancing their precision. The application range of integrated photonic systems is constantly expanding to areas including trapped-ion quantum computers (QCs) [1, 2, 3], quantum sensing with trapped ions [4] and neutral atoms [5, 6], as well as quantum communication [7]. Current approaches to govern and focus laser light for optical addressing typically rely on the use of bulk optics, leading to undesired influences on the fidelity of operations and preventing further scalability [1]. Circumventing the large bulk optics and providing the optical requirements of the atoms, in terms of wavelength and intensity, require an accurate simulation, fabrication, and characterization of the integrated on-chip systems. Especially for QCs with ions as qubits, the preparation and operation of atoms require addressing multiple ion transitions with linearly and circularly polarized light in a broad range of wavelengths, from UV to NIR. This can be accomplished by Si_3N_4- and AlN-based integrated waveguides (WGs) and grating couplers (GCs), providing an efficient solution for flexible on-chip light routing with a small footprint and integration ability with the trap electrodes. In addition, integrated optics for multi-wavelength operation help to enhance the robustness of on-chip light guidance and increase the scalability of quantum chips for a wide range of trapped ion architectures.

Here, we present and numerically demonstrate a WG and focusing GCs for optical ion addressing at the wavelengths of $\lambda_1 = 760\ \mathrm{nm}$ and $\lambda_2 = 935\ \mathrm{nm}$ based on the Si_3N_4/SiO_2 material platform. The structures are designed for linearly polarized light with predefined figures of merit, like focused beam sizes ($\omega_0 = 2 - 30\ \mu\mathrm{m}$) and emission angles ($\vartheta_{\mathrm{em}} = -75°$ to $75°$). Fig. 1 left shows the schematic overview of the GCs integrated within the ion trap, and Fig. 1 right schematically demonstrates the WG and GC system in more detail. The electrodes create a trapping potential above the chip surface, and the optical components allow addressing multiple transitions to prepare and control the ion-qubits.

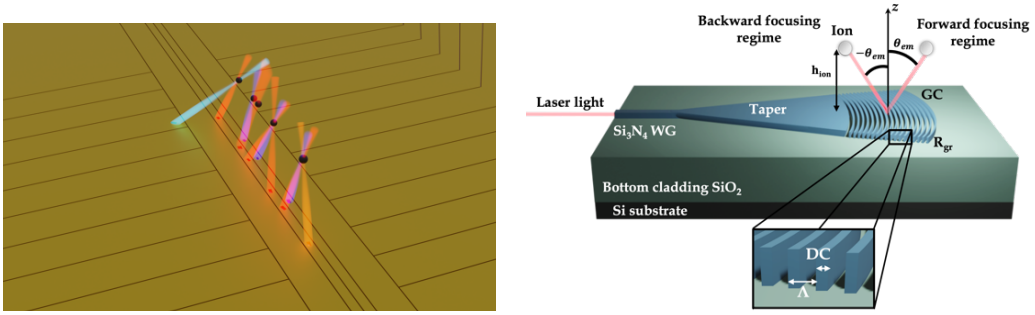

Fig. 1 left: Schematic view on the trapped-ion QC chip with circular- and elliptic beam shapes, right: WG-GC design scheme with forward and backward light focusing regimes.

RESULTS AND DISCUSSION

Single-mode waveguide for NIR

The finite-difference eigenmode (FDE) solver of Lumerical MODE was utilized to evaluate single-mode (SM) and multi-mode (MM) regimes for different Si_3N_4/SiO_2 WG geometries at λ_1 and λ_2. Nested sweeps of the core width w_{core} and the core height h_{core} have been performed to investigate the modal confinement and the modal polarization purity of the fundamental quasi-TE and quasi-TM modes, respectively. Fig. 2 left shows the modal effective refractive index n_{eff} of quasi-TE_{00} mode in the SM regime at $\lambda_1 = 760\ \mathrm{nm}$. SM WG geometries with large $w_{\mathrm{core}}/h_{\mathrm{core}}$ - ratios offer a very high modal polarization purity but suffer from lower mode confinement. To further expand the functionality of the WGs for scalable light routing on-chip and enable a multi-wavelength operation with $\lambda_2 = 935\ \mathrm{nm}$ in the same WG, a reasonable mode confinement factor at the longer wavelength has been considered in the choice of the WG geometry. Therefore, the WG geometry $520 \times 200\ \mathrm{nm}^2$ was chosen to support a moderately high confined quasi-TE_{00} mode with high mode polarization purity and suppression of weakly guided quasi-TM_{00} mode. Although the WG is on the border of the SM regime, the higher order mode is near cut-off and is therefore expected to be extinguished by high bending losses in WG bends.

Additionally, the FDE solver was used to investigate WG bends (see Fig. 2 right). The total mode-mismatch loss of the input and output interfaces L_{MM} and the radiation loss $L_{\mathrm{rad.}}$ have been simulated at different bending radii r_{bend} at both wavelengths for the quasi-TE_{00} mode of the chosen WG geometry. Subsequently, the total bending losses $L_{\mathrm{bend,tot.}}$ were calculated using estimated propagation losses $L_{\mathrm{propag.}}$. Based on experimental data, a propagation loss per unit length $\alpha_{\mathrm{propag.}} = 0.75\ \mathrm{dB/cm}$ was assumed for $\lambda_2 = 935\ \mathrm{nm}$ [8]. Due to the decreased mode confinement, the longer wavelength dictates the limitations of the bending radius. A minimum total loss of $L_{\mathrm{bend,tot.}} = 0.013\ \mathrm{dB}$ can be achieved by a radius of $r_{\mathrm{bend}} = 60\ \mu\mathrm{m}$. For even more compact light routing on-chip, we have implemented WG bending radius of $r_{\mathrm{bend}} = 20\ \mu\mathrm{m}$, where minor losses of $L_{\mathrm{bend,tot}} = 0.09\ \mathrm{dB}$ are expected.

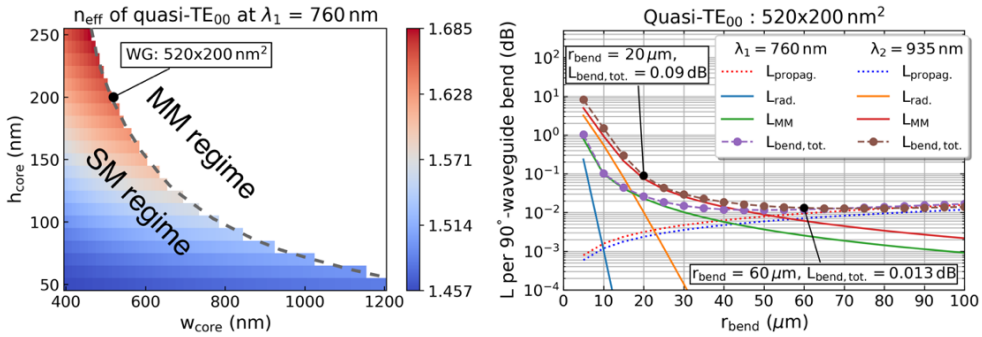

Fig.2 left: Nested parameter sweep results for $n_{\mathrm{eff}} = f(w_{\mathrm{core}}, h_{\mathrm{core}})$ of quasi-TE_{00} at $\lambda_1 = 760\ nm$, right: losses of a 90°-waveguide bend in dB of quasi-TE_{00} at $\lambda_1 = 760\ nm$ and $\lambda_2 = 935\ nm$.

Focusing grating coupler in forward and backward regimes

The in-coupled laser light is guided by the WG and extended by the taper to the area of the GC. Control over emission angle (ϑ_{em}) and grating strength are maintained by nonlinear apodization of grating period (Λ) and duty cycle (DC). Altering the radius of the GC (R_{gr}) leads to a Gaussian beam profile with a well-controlled focused beam size at the position of the trapped ion. The described design concept has been applied, and the produced near- and far-field were studied using a finite-difference time-domain solver (FDTD) of Lumerical FDTD. Forward and backward focusing regimes for light delivery have been considered (see Fig. 3). By choosing relatively large Λ and DC, forward focusing enables the generation of a focused µm-beam while maintaining the manufacturing constraints. However, additional intensity peaks due to higher-order diffraction require further optimization of a full-layer chip to minimize the parasitic influence of scattered light on the ion. In contrast, the backward focusing regime can suppress undesired higher-order diffraction but yields a trade-off concerning fabrication limits. The presented GC designs allow controlling beam parameters independently in the longitudinal (LD) and transversal (TD) directions of the light propagation, bringing the light above the surface in circular- and elliptical shapes. Therefore, GCs can be used for addressing not only a single trapped ion with minimum beam crosstalk but also a chain of the trapped ions by keeping the small beam radius in LD and enlarging it in TD, as shown in Fig. 3A. Additionally, we have optimized the design of the WG and GC system in such a way that by using the same structure, light confinement and a beam overlap can be achieved for λ_1 and λ_2 simultaneously. Thus, we can substantially minimize the number of optical components on the chip by addressing two transitions in the same ion concurrently.

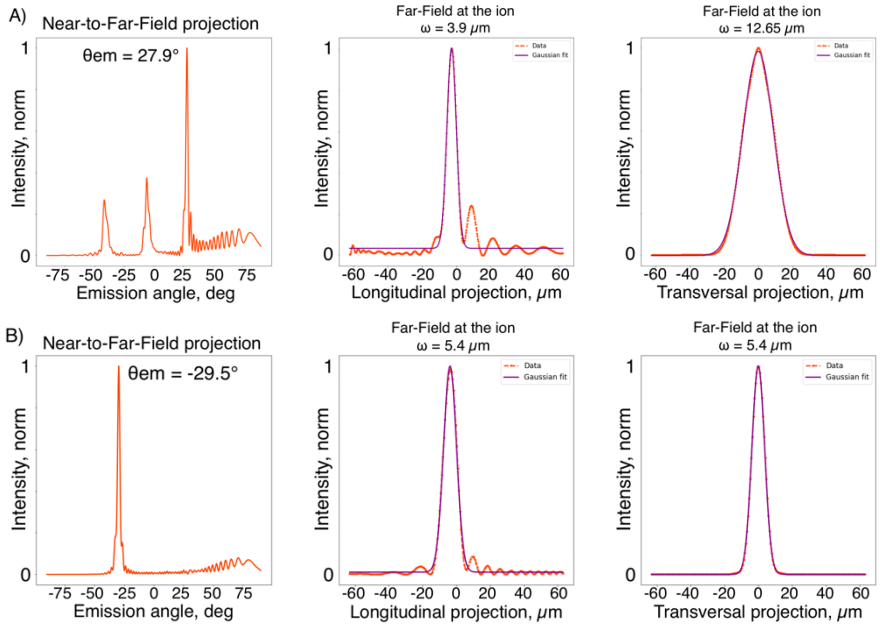

Fig. 3. Optical far-field characteristics of the GC in A) forward regime ($\vartheta_{em} = 27.9°$) with an elliptical beam shaping, where $\omega_{0,LD} = 3.9\ \mu m, \omega_{0,TD} = 12.65\ \mu m$ and B) backward focusing regime ($\vartheta_{em} = -29.5°$) with a spherical beam shaping, where $\omega_{0,LD} = \omega_{0,TD} = 5.4\ \mu m$. The ion position is 100 μm above the chip surface.

Moreover, we have evaluated the designed GCs efficiency and the influence of the layers on the focused beam. Hence, the total percentage of light reaching the ion above the chip surface can be expressed in the following way:

$$T = \frac{\frac{1}{2}\int_{\text{GC area}} Re\{\vec{P}\}\mathrm{d}\vec{S}}{P_{\text{in}}} \cdot 100, \tag{1}$$

where $\vec{P}$ is the Poynting vector, P_{in} is the input power coupled into the WG, and the GC area is an area above the GC in the near-field. Thereby, the simulated light efficiency in the near-field with the presence of SiO_2 layers is almost $T = 50\ \%$, and the efficiency in the near-field with all layers can drop down to $T \approx 30\ \%$. Due to the presence of multiple layers, such as a transparent conductive coating (ITO) and air, a multitude of interference mechanisms as well as reflections and refraction can occur. This substantially affects the overall optical performance of the device. However, in the framework of our trapped-ion chip design, the beam characteristics are rather prevalent. Further optimization of the GC performance can be accomplished by breaking the symmetry of the structure and varying the etching depth.

OUTLOOK

Based on the insights yielded from our design studies, we are extending the optical control to other polarization states, such as left and right circularly polarized light. Transferring the applied concepts towards the UV regime, we aim to utilize the advantages of AlN material to address transitions for photoionization, cooling and detection. The fabricated structures are then characterized by a near-field beam profiling setup to verify the numerical results and to encourage further design iterations toward higher beam-shaping features.

Acknowledgments: The authors gratefully acknowledge support by B-IGSM and the DFG Research Training Group GrK1952/1 “Metrology for Complex Nanosystems”. We thank the Quantum Valley Lower Saxony, ATIQ and the cluster of Excellence Quantum Frontiers (EXC-2123 – 390837967).

References

[1] C. Bruzewicz, *Trapped-ion quantum computing: Progress and challenges*, APR, vol. 6, no. 2, p. 021314, 2019
[2] K. Mehta, *Integrated optical multi-ion quantum logic*, Nature, vol. 586, no. 7830, pp. 533-537, 2020
[3] R. Niffenegger, *Integrated multi-wavelength control of an ion qubit*, Nature, vol. 586, no. 7830, pp. 538-542, 2020
[4] M. Day, *A micro-optical module for multi-wavelength addressing of trapped ions*, QST, vol. 6, no. 2, p. 024007, 2021
[5] A. Isichenko, *Photonic integrated beam delivery in a rubidium 3D magneto-optical trap*, arXiv: 2212.11417, 2022
[6] A. Ferdinand, *A scalable infrastructure for strontium optical clocks*, CLEO: Science and Innovations, pp. STu5O-1, 2022
[7] G. Moody, *2022 Roadmap on integrated quantum photonics*, Journal of Physics: Photonics, vol. 4, no. 1, p. 012501, 2022
[8] A. Subramanian, *Low-loss singlemode PECVD silicon nitride photonic wire waveguides for 532–900 nm wavelength window fabricated within a CMOS pilot line*, IEEE Photonics Journal, vol. 5, no. 6, pp. 2202809-2202809, 2013